Desalination and Water Treatment
www.deswater.com

doi: 10.1080/19443994.2016.1155173

57 (2016) 25830–25841
November

Taylor & Francis
Taylor & Francis Group

Preparation and characterization of magnetic Fe_3O_4@sulfonated β-cyclodextrin intercalated layered double hydroxides for methylene blue removal

Wenjihao Hu[a], Xia Wu[a], Feipeng Jiao[a,*], Weijie Yang[b,*], Yangmeihui Zhou[a]

[a]*School of Chemistry and Chemical Engineering, Central South University, Changsha 410083, P.R. China, Tel./Fax: +86 731 88830833; email: jiaofp@163.com (F. Jiao)*
[b]*School of Chemistry and Chemical Engineering, Zhoukou Normal University, Zhoukou 466001, P.R. China, Tel./Fax: +86 731 88830833; email: chemsnow@163.com*

Received 18 June 2015; Accepted 6 February 2016

ABSTRACT

Nanocage structures derived from sulfated β-cyclodextrin (SCD) intercalated MgAl layered double hydroxides ($MgAl\text{-}NO_3$ LDHs) were prepared through ion-exchange reactions. Coprecipitation method was used to prepare the composites of magnetic Fe_3O_4@sulfonated β-cyclodextrin intercalated LDH (Fe/SCD-LDH), which was demonstrated having an efficient adsorption capability to cationic pollutants and an excellent reuseability. X-ray diffraction and Fourier transform infrared spectroscopy confirmed that SCD was intercalated successfully and the basal spacing was expanded to 1.63 nm. N_2-adsorption/desorption and scanning electron microscopy displayed that the resulting Fe/SCD-LDH possessed high crystallinity, hierarchical structure as well as large specific surface area. Energy-dispersive X-ray spectroscopy was used to investigate the type and content of the elements in Fe/SCD-LDH. Batch adsorption experiments were carried out to investigate the removal of methylene blue (MB) from aqueous solution using Fe/SCD-LDH as the adsorbent. MB was selected owing to its toxic and carcinogenic features as a kind of cationic dye. The adsorption process could be well described by the pseudo-second-order kinetic model and fitted well with the Langmuir isotherm model.

Keywords: Layered double hydroxides; Sulfated β-cyclodextrin; Magnetic iron oxide; Removal; Methylene blue

1. Introduction

The removal of dyes from wastewater is a current issue for both foundational research and practical applications [1,2]. Dye contamination in industrial wastewater, resulting from textiles, paper, printing, plastics, leather, and so on, has become a major concern because of their adverse effects to many forms of life. The discharge of dyes into the environment is a matter of concern for both toxicological, carcinogenic hazard on human being and esthetical influence on environment. Recently, the removal of dye from aqueous solutions via adsorption has attracted much attention due to its efficiency, economic feasibility, simplicity of design, recycle of adsorbent, and no secondary pollution [3,4]. The key problem for fundamental and practical applications of adsorption, however, is to find an efficient adsorbent.

*Corresponding authors.

Layered double hydroxides (LDHs), a class of anionic clays, consist of positively charged brucite-like layers and interlamellar exchangeable anions [5]. The LDHs can be described by the general formula: $\left[M^{2+}_{1-X}M^{3+}_{X}(OH)_2\right]^{x+}(A^{n-})_{x/n}\cdot mH_2O$, where M^{2+} and M^{3+} are divalent and trivalent cations respectively, occupying octahedral positions in the brucite-like layer; M^{2+} can be Mg, Zn, Fe, or Co and M^{3+} can be Al, Cr, Fe, or Mn; x is equal to the molar ratio of $M^{2+}/(M^{2+} + M^{3+})$ and ranges from 0.17 to 0.33; A^{n-} is an interlayer charge-compensating anion, such as Cl^-, NO_3^-, CO_3^{2-}, and SO_4^{2-} [6]. Recently, extensive investigations have been carried out to study the LDHs because of the relatively large surface areas (20–120 m^2/g) and a wide variety of charge-balancing anionic species into the gallery region [7,8]. Furthermore, because of easy preparation, low cost, full protection for the intercalated molecules, high suitability and low toxicity, LDHs are superior to other clay minerals [9,10]. Therefore, LDHs are considered as potential adsorbents and ion exchangers and their extensive intercalation chemistry has widespread applications in areas such as anion exchangers [11], acid absorbents [12], bioactive nanocomposites [13], catalysts [14], catalyst precursors [15], electroactive and photoactive materials [16]. However, many of the applications are largely restricted due to the intercalated of molecules or ions must be negative. Besides, like most of adsorbents, LDHs as powder materials are very difficult to be separated and collected.

SCD, as a kind of negatively charged cyclodextrins, has been widely applied to enantiomeric separation, either by liquid chromatography using columns containing the materials bound to a solid support or by capillary electrophoresis [17]. It can interact with guest molecules selectively to form inclusion complexes based on the size, shape, polarity, and various interactions such as van der Waals, dipole–dipole interactions, and hydrogen bonding. The combination of high hydrophilic SCD with LDHs may broaden the adsorption species of LDHs and make up the defect that LDHs are usually inclined to adsorb anionic dyes.

Concerning to the difficult separation and collection of LDHs, magnetic iron oxide (Fe_3O_4) may be a promising candidate material, which has a good recycled property via an external magnetic field, with no secondary pollutants produced. Moreover, Fe_3O_4 is environmental friendly and easily synthesized.

In this work, we presented a simple method to synthesize a kind of SCD-LDHs, which was then loaded with Fe_3O_4 to improve the recycled ability. The structural, morphological, and textural properties of as-synthesized solids were confirmed by X-ray diffraction (XRD), N_2-adsorption/desorption, vibrating sample magnetometer (VSM), scanning electron microscopy (SEM), energy-dispersive X-ray spectroscopy (EDX), and Fourier transform infrared spectroscopy (FT-IR) methods. Methylene blue (MB) was selected as a kind of alkaline wastewater in this study to evaluate the adsorption capabilities. The effects of contact time, pH, the initial concentration of MB, and temperature were investigated to establish the optimum adsorption conditions. Desorption and regeneration experiment was also studied to show the recycled ability. In addition, the isotherms and kinetics were explored to describe the experimental data.

2. Experimental

2.1. Materials

$Mg(NO_3)\cdot 6H_2O$, $Al(NO_3)\cdot 9H_2O$, $NaNO_3$ and $FeCl_3\cdot 6H_2O$ were purchased from Kemiou Chem. Co. Ltd (Tianjing, China). NaOH and anhydrous sodium acetate were obtained from Taishan Chem. Co. Ltd (Guangzhou, China). HNO_3, ethanol and ethylene glycol were analytical grade and commercially available products. PEG (2000) was selected from Sinopharm Chem. Co. Ltd. (Shanghai, China). β-cyclodextrin, sulfated sodium salt (SCD), supplied from Aldrich Chem. Co. Ltd (USA) was used without further purification. MB (C.I. number = 319.86, molecular formula = $C_{16}H_{18}ClN_3S$, λ_{max} = 664 nm) was purchased from Beijing Chemical Works (Beijing, China) and was used without further purification. All other chemicals were of analytical-reagent grade and water was deionized and bidistilled.

2.2. Synthesis

2.2.1. Synthesis of MgAl-NO_3 LDH

Mg/Al-NO_3 LDH was prepared in 2:1 M rations by the classic coprecipitation method [18]. Briefly, a solution containing 0.03 mol of $Mg(NO_3)\cdot 6H_2O$ and 0.015 mol of $Al(NO_3)\cdot 9H_2O$ was added dropwise to a magnetically stirred solution containing 2.2 mol of NaOH and 0.667 mol of $NaNO_3$. The solution pH was maintained slightly higher than 10. The mixture was aged at 353 K for 24 h. The obtained gel was washed with deionized water till neutral pH, and the resulting mixture was separated by filtration. Subsequently, the obtained sample was dried in a vacuum oven at 353 K overnight.

2.2.2. Synthesis of SCD-LDH

The composite of SCD-LDH was obtained by an ion exchange method as follows: 1.2 g SCD was

dissolved in 50 mL of deionized water, which was then added into 50 mL of a suspension of the prepared Mg/Al-NO_3 LDH (0.5 g). The mixture solution was stirred under nitrogen atmosphere at 373 K for 24 h. It was then centrifuged and washed several times with deionized water. The obtained compound was donated as SCD-LDH.

2.2.3. Synthesis of Fe/SCD-LDH

The magnetic particle Fe_3O_4 was prepared by means of a solvothermal reaction as reported previously [19]. Briefly, 2.025 g $FeCl_3{\cdot}6H_2O$ was added to 60 mL ethylene glycol solution. Then, 5.4 g anhydrous sodium acetate and 1.5 g PEG (2000) were added to the solution. After all, the solid was dissolved; the mixed solution was transferred into a Teflon stainless steel autoclave, sealed, and heated at 473 K for 8 h. The resulting black magnetite particle was separated by putting the vessel on an Nd–Fe–B permanent magnet and washed several times with ethanol. Subsequently, the obtained sample was dried in a vacuum oven at 353 K overnight.

To obtain the Fe/SCD-LDH composite, 0.15 g Fe_3O_4 and 0.5 g SCD-LDH were dispersed in 60 mL deionized water, and then ultrasonicated for 30 min. The mixture was then transferred into a Teflon stainless steel autoclave and heated at 423 K for 5 h. The resulting composite was washed several times with deionized water. Finally, the obtained sample was dried in a vacuum oven at 353 K for 24 h.

2.3. Characterization

The XRD patterns were recorded on a powder X-ray diffractometer (Bruker D8), using Cu Kα (λ = 1.5406 Å) radiation at voltage 40 kV and current 40 mA. The samples were scanned in steps of 0.04° (2θ) in the range of 3–70° with a count time of 4 s per step. FT-IR spectra were collected with a Nicolet Avatar 360 spectrophotometer. The sample was finely ground, mixed with an oven-dried spectroscopic grade KBr, and pressed into a disc. The spectrum of each sample was scanned at 2 cm^{-1} resolution between 400 and 4,000 cm^{-1}. SEM images were obtained using a JEOL JSM-6360LV microscope. EDX spectroscopy was used to investigate the chemical composition of the samples. The BET surface areas of samples were calculated from N_2 adsorption/desorption experiments determined at 77 K using a Quantachrome Autosorb-1 system. Concentrations of MB were analyzed by a spectrophotometer UV-2802S. The magnetic properties were analyzed with a VSM (LDJ 9600-1, USA).

2.4. Adsorption experiments

The adsorption study was investigated by batch experiments. In general, 0.1 g adsorbent was added to 100 mL of MB solution with a certain concentration. The mixture was agitated in a temperature-controlled shaking water bath at a constant speed of 180 rpm. Effects of contact time (0–5 h), solution pH (4.0–11.0), temperature (283, 293, 303 and 313 K), and initial MB concentration (40–160 mg/L) on the adsorption were investigated. After adsorption, the adsorbent was magnetically removed using a strong permanent magnet made of Nd–Fe–B. The residual concentration of MB in the supernatant was determined at 664 nm, and the quantity of MB adsorbed by Fe/SCD-LDH was calculated using the following equation:

$$Q = \frac{(C_0 - C_t)V}{m} \quad (1)$$

where Q is the adsorption capacities (mg/g), C_0 and C_t are the initial and final concentrations of MB (mg/L), respectively. V is the volume of MB solution (L) and m is the adsorbent dosage (g).

To investigate the reusability of the prepared adsorbent, desorption and regeneration experiments were conducted using deionized water as eluents under ultrasonic irradiation. The Fe/SCD-LDH after desorption treatment was rinsed till neutral pH and dried in a vacuum oven at 353 K overnight. Then, it was reused for MB removal at the same adsorption conditions.

3. Results and discussion

3.1. Characterization of samples

3.1.1. XRD analysis

The XRD patterns of MgAl-NO_3 LDH, SCD-LDH, and Fe/SCD-LDH are shown in Fig. 1, and their basal spacing and lattice parameters values are listed in Table 1. The XRD pattern of MgAl-NO_3 LDH (Fig. 1(a)) showed four characteristic peaks at 2θ = 10.26°, 21.22°, 31.80°, and 60.74°, which fitted well to the crystal planes of (0 0 3), (0 0 6), (0 0 9), and (1 1 0) of crystalline LDH, respectively [20]. This confirmed the formation of crystallized layered compounds. The basal spacing of MgAl-NO_3 LDH calculated from the (0 0 3) diffraction was 0.86 nm and also identical to the value reported in the literature [21]. As shown in Fig. 1(b), SCD-LDH showed obvious shift in the (0 0 3) reflection to lower angle, suggesting that the SCD had been successfully intercalated into the

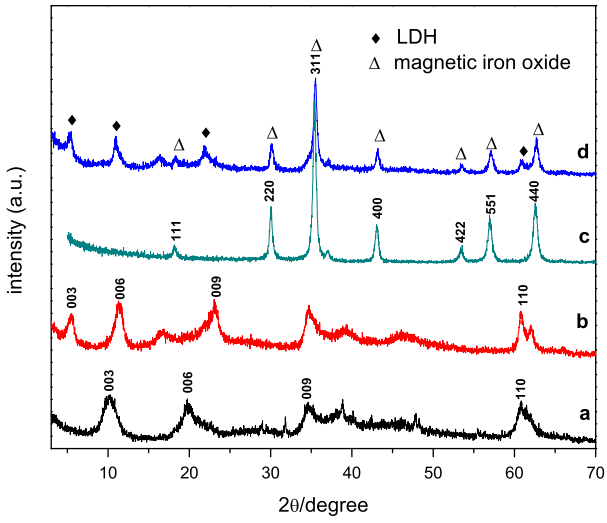

Fig. 1. XRD patterns for MgAl-NO_3 LDH (a), SCD-LDH (b), Fe_3O_4 (c) and Fe/SCD-LDH (d).

LDHs. The same phenomenon also appeared on the pattern of Fe/SCD-LDH (Fig. 1(d)). Fig. 1(c) is the XRD pattern of Fe_3O_4 (JCPDF 97-007-7588). The characteristic reflections of LDH and Fe_3O_4 confirmed that Fe_3O_4 was loaded on intercalated LDH successfully.

Moreover, as shown in Table 1, the values of lattice parameter remained almost constant (0.304 nm) for LDH, SCD-LDH, and Fe/SCD-LDH, indicating that there was no significant change in the average distance between the metal ions and Mg^{2+}/Al^{3+} ratio after the SCD intercalated. The basal spacing expanded to 1.63 nm, when NO_3^- was replaced by SCD anion in an ion exchange reaction. As the thickness of the LDH layer was 0.48 nm, the gallery height corresponding to the (0 0 3) peaks in SCD-LDH and Fe/SCD-LDH was thus 1.15 nm, which was much smaller than the double of the torus thickness (0.78 nm × 2) and one outer diameter (1.53 nm) of β-CD. Thus, the results inferred that SCD had been intercalated into the gallery with their cavity axes perpendicular [22].

3.1.2. FT-IR analysis

The FT-IR spectra of SCD, MgAl-NO_3 LDH, SCD-LDH, and Fe/SCD-LDH are shown in Fig. 2. The broad absorption bands at 3,450 and 1,642 cm^{-1} correspond to the stretching vibration of the hydroxyl group and physically adsorbed water molecules. For SCD (Fig. 2(a)), the obvious absorption band at 2,959 cm^{-1} can be assigned to the stretching vibration of $-CH_2$ of β-CD skeleton. The peaks at 1,260 and 1,056 cm^{-1} in SCD (Fig. 2(a)) were due to the asymmetric stretching vibrations of SO_2 and S–O, while those at 1,157, 1,024, and 942 cm^{-1} were attributed to the absorption of C–O, C–O–C of glucose units and C–O–C of the rings, respectively [23]. The intense band of MgAl-NO_3 LDH (Fig. 2(b)) at 1,380 cm^{-1} was assigned to the asymmetric and symmetric stretching vibrations of interstratified NO_3^-, in good agreement with the XRD result (Fig. 1(a)). Moreover, the peak at 665 cm^{-1} was due to the lattice valence vibration of Mg–O [24]. In the SCD-LDH and Fe/SCD-LDH composites (Fig. 2(c) and (d)), characteristic bands at 1,260 and 1,056 cm^{-1} were also observed, which provided further evidence for the introduction of SCD into the LDH. Furthermore, the peak at 551 cm^{-1} in Fig. 2(d) corresponded to the Fe-O vibration of magnetite phase, consistent well with XRD result (Fig. 1d).

3.1.3. SEM and EDX analysis

SEM was employed to investigate the morphological and microstructural details of the as-prepared particles. The results are shown in Fig. 3. The particles like irregular platelets in Fig. 3(A) were LDHs, which

Table 1
Lattice parameters of as-prepared composites

	MgAl-NO_3 LDH		SCD-LDH		Fe/SCD-LDH	
Diffraction peaks	2θ (°)	d (nm)	2θ (°)	d (nm)	2θ (°)	d (nm)
0 0 3	10.26	0.862	5.52	1.63	5.44	1.63
0 0 6	21.22	0.418	11.38	0.777	10.98	0.805
0 0 9	31.80	0.281	23.18	0.529	21.80	0.548
1 1 0	60.74	0.152	60.78	0.152	60.82	0.152
Lattice parameter a	0.304 nm		0.304 nm		0.304 nm	
Lattice parameter c	2.585 nm		4.800 nm		4.902 nm	

Notes: $a = 2d(1\ 1\ 0)$, $c = 3d(0\ 0\ 3)$.

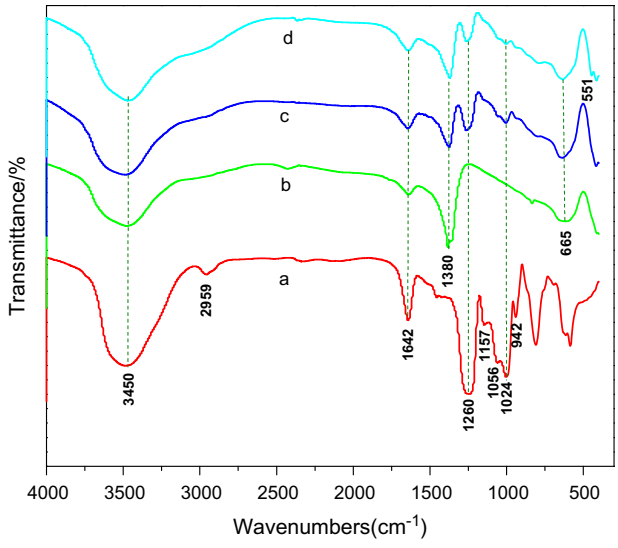

Fig. 2. FT-IR spectra of SCD (a), MgAl-NO_3 LDH (b), SCD-LDH (c) and Fe/SCD-LDH (d).

were crystallites and uniformity in nature. This could be attributed to a homogeneous and slow nucleation process [25]. After SCD intercalated, no change occurred on morphology (Fig. 3(B)). From Fig. 3(C), the spherical nanometer microspheres with an average size of 200 nm were Fe_3O_4. Furthermore, these particles were uniform and dispersed well. Fig. 3(D) reflected that the loaded Fe_3O_4 particles were uniformly embedded into the entire MgAl-NO_3 LDH frame, including the surface, internal, and external walls of the LDH. Table 2 summarized the obtained EDX analysis data for LDH, SCD-LDH, and Fe/SCD-LDH. It can be seen that the proportion of S element is 3.59%. It determined the amount of SCD intercalated in LDH.

3.1.4. Magnetic property analysis

The room temperature magnetization curves in Fig. 4 showed similar shape but different saturation magnetizations (M_s) in the range of 78.78–24.49 emu/g. Fe/SCD-LDH (Fig. 4(b)) exhibits a ferromagnetic behavior of the composite with value of M_s about 34.23 emu/g. Compared to Fig. 4(a), the decrease of M_s in Fe/SCD-LDH was due to its larger content of non-magnetic LDH phase. After MB adsorbed, the M_s of Fe/SCD-LDH turned to 24.49 emu/g (Fig. 4(c)). All the magnified hysteresis loops further confirmed the superparamagnetism of these particles. The magnetic separability of such a magnetic composite was tested in deionized water by placing a magnet near the glass.

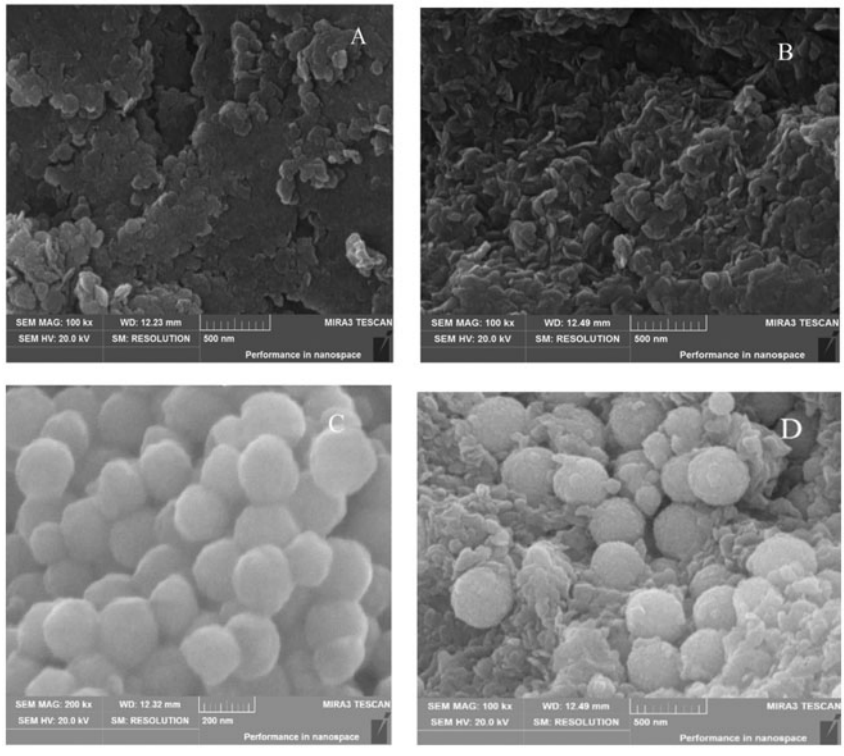

Fig. 3. SEM images of MgAl-NO_3 LDH (A), SCD-LDH (B), Fe_3O_4 (C) and Fe/SCD-LDH (D).

Table 2
Elemental analysis data of the synthesized nanomaterials obtained from EDX

Sample	Mg (%)	Al (%)	Fe (%)	C (%)	N (%)	O (%)	S (%)
MgAl-NO_3 LDH	24.97	13.50	–	5.82	12.85	40.99	–
SCD-LDH	15.85	8.22	–	27.83	2.24	33.16	7.80
Fe/SCD-LDH	7.40	4.02	19.88	18.59	1.11	34.54	3.59

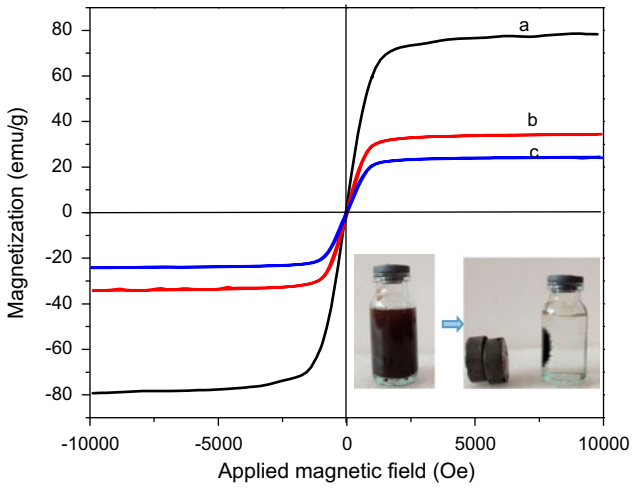

Fig. 4. Room-temperature (298 K) magnetic hysteresis loops of Fe_3O_4 (a), Fe/SCD-LDH (b) and Fe/SCD-LDH after MB is adsorbed (c).

Compared with more than 30 min for completely gravity sedimentation of LDH, rapid magnetic separation of Fe/SCD-LDH was achieved in 5 s (inset in Fig. 4). Therefore, separation of the as-fabricated Fe/SCD-LDH composite rapidly becomes positive for the environmental protection due to the recycled property.

3.1.5. N_2 adsorption/desorption analysis

The results of N_2 adsorption/desorption experiment for Fe/SCD-LDH and LDH are shown in Fig. 5. Fe/SCD-LDH had the isotherms of type IV with the hysteresis loop of type H3 (Fig. 5(A)), which characterized mesoporous solid according to the IUPAC classification. This type of hysteresis loop was attributed to the slit-shaped pores generated by the aggregation of plate-like particles [26]. The surface area derived from the N_2 adsorption/desorption isotherms for Fe/SCD-LDH is 37.85 m^2/g, while the related average pore diameter value is 12.28 nm. By comparison, the surface area of LDH derived from the N_2 adsorption/desorption isotherms in Fig. 5(b) is 13.23 m^2/g and the average pore diameter value is 1.94 nm. According to the BET theory, the surface area of Fe_3O_4 is 67.24 m^2/g and it is 32.29 m^2/g for SCD-LDH. Compared with the surface area of Fe/SCD-LDH, Fe_3O_4 and SCD increased the surface area of the adsorbent.

3.2. Adsorption of MB onto Fe/SCD-LDH

3.2.1. Effect of pH

The effect of initial solution pH on the adsorption of MB onto Fe/SCD-LDH was carried out at different pH between 4.0 and 11.0, 303 K, and the initial MB concentration was 120 mg/L. As shown in Fig. 6, the adsorption amount increased with the increase in the pH value from 4.0 to 7.0. Due to the strong hydrophilic at low pH, MB molecules may have weak interaction with hydrophobic cavity of SCD. When the initial pH value ranged from 7.0 to 10.0, the adsorption amount slightly reduced. However, when the pH was above 10.0, the adsorption capacities increased since MB molecules with ammonium salt were neutralized and the interaction between neutral MB and the cavity of SCD was strengthened. As the adsorption amount of MB remained almost same at pH 7.0–10.0, the following studies were conducted at a neutral pH.

3.2.2. Effect of contact time

Fig. 7 shows the effect of contact time on MB removal by Fe/SCD-LDH, LDH, Fe_3O_4, and SCD adsorption experiments were carried out at time intervals ranging from 0 to 5 h at 303 K, pH 7.0. The adsorption capacity of MB by Fe/SCD-LDH increased with the contact time and reached the equilibrium in a short time. It had a strong adsorption capacity of 85.26 mg/g. Besides, the adsorbed amount of MB was much higher than that by LDH, Fe_3O_4, and SCD. Since LDH usually inclined to adsorb anions, however, MB was a cationic dye. This indicated that SCD played an important role in the adsorption process. Fe/SCD-LDH, with the hydrophobic cavity of SCD, could improve the range of selective adsorption of LDH

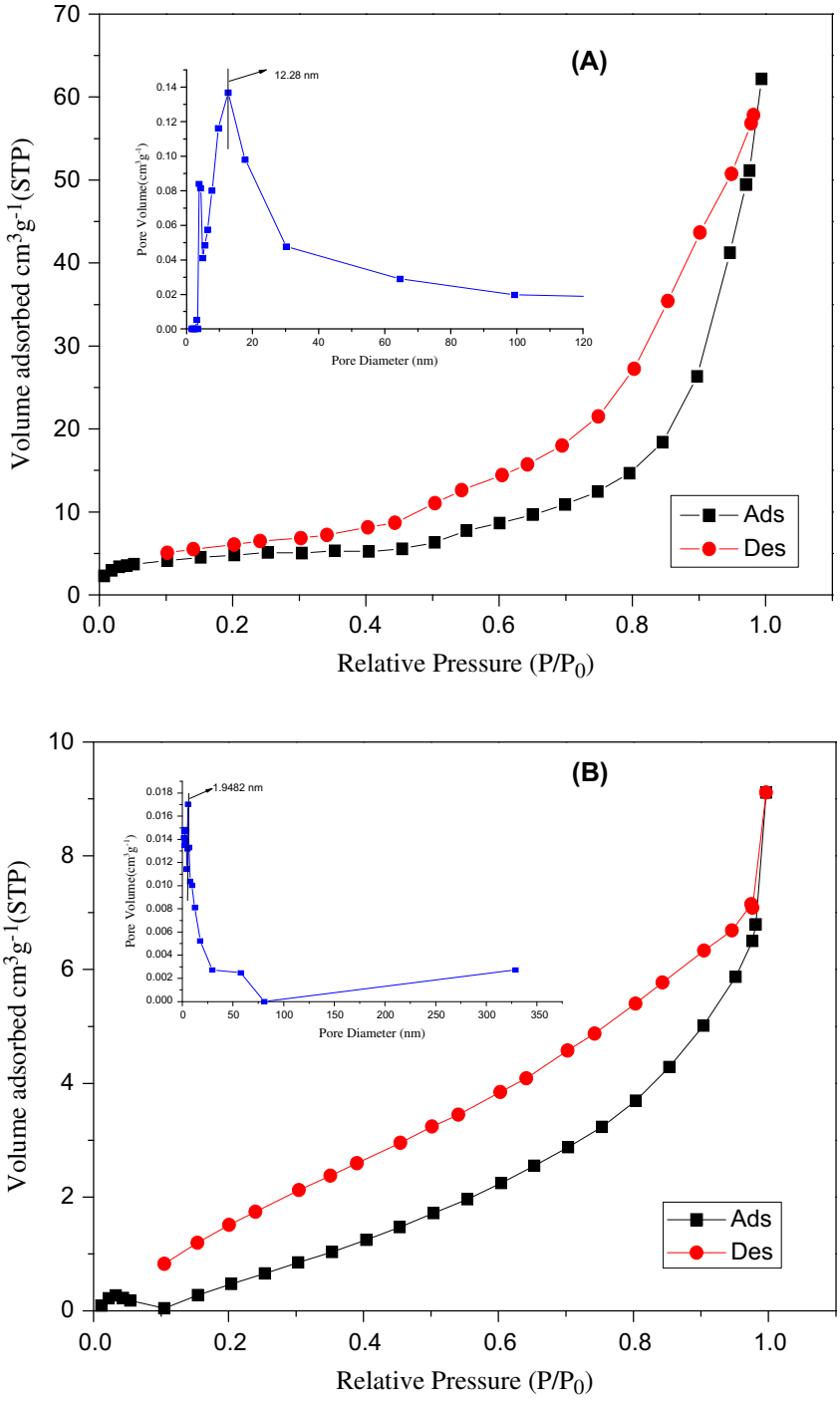

Fig. 5. N_2-adsorption/desorption isotherm and corresponding pore size distribution of Fe/SCD-LDH (A) and LDH (B).

effectively. It can be seen in Fig. 7 that the adsorption rate of MB by Fe/SCD-LDH was high in the first 30 min. Due to the aggregation of MB and the increasing of the electrostatic repulsion, the adsorption rate then became slow. After about 2 h, the adsorption equilibrium reached. To be mentioned, the adsorption capacity of MB by SCD-LDH was higher than that by Fe/SCD-LDH. However, Fe/SCD-LDH could be solved the difficult separation and collection of SCD-LDH and improved the recycled ability.

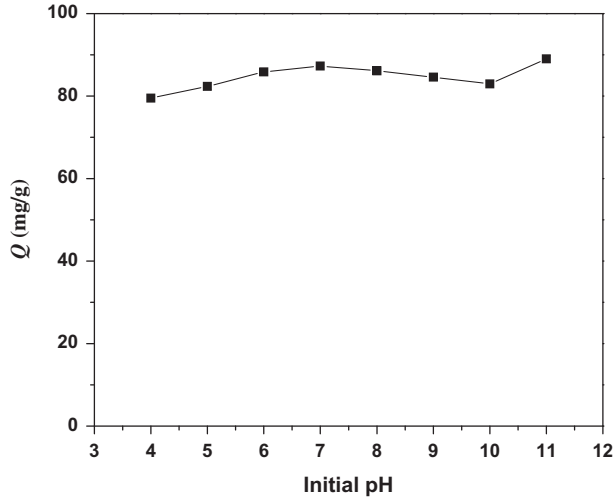

Fig. 6. Effect of pH on the adsorption of MB by Fe/SCD-LDH (conditions: initial MB concentration: 120 mg/L, volume: 100 mL, temperature: 303 K, adsorbents: 0.1 g).

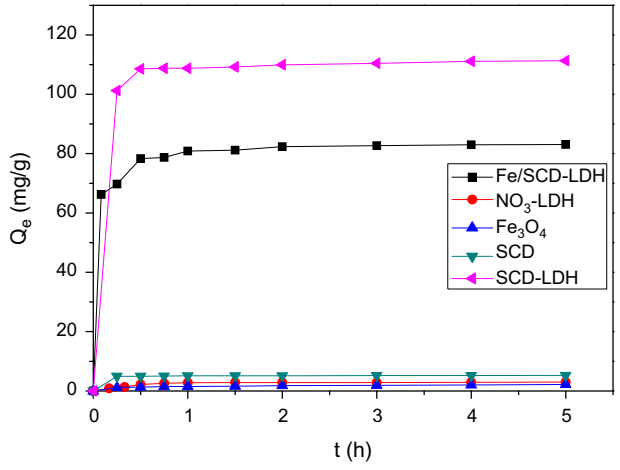

Fig. 7. Effect of contact time on the adsorption of MB by Fe/SCD-LDH, LDH, Fe_3O_4, SCD, and SCD-LDH (conditions: volume: 100 mL, adsorbents: 0.1 g, temperature: 303 K, pH 7).

3.2.3. Effect of initial concentration

The effect of initial concentration on the adsorption of MB by Fe/SCD-LDH was carried out at initial MB concentration ranging from 40 to 160 mg/L at 303 K, pH 7.0. It can be observed from Fig. 8 that the equilibrium adsorption capacity of MB increased with the increase in initial MB concentration. However, the removal rate of MB presented an obvious decline at the MB concentration ranged from 120 to 160 mg/L, owing to the limitation of adsorbent dose. MB was removed very fast especially at low initial concentrations. The largest amount of dye adsorbed to the composite within approximately 30 min suggested the possibility to form monolayer coverage of MB at the outer interface of Fe/SCD-LDH. This confirmed that Fe/SCD-LDH could rapidly and effectively adsorb MB from aqueous solution.

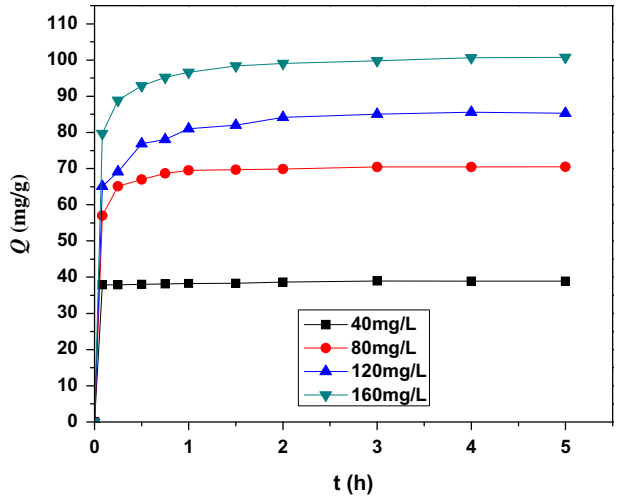

Fig. 8. Effect of initial concentration on the adsorption of MB by Fe/SCD-LDH (conditions: volume: 100 mL, adsorbents: 0.1 g, contact time: 5 h; temperature: 303 K, pH 7).

3.2.4. Desorption and regeneration experiment

The effect of consecutive adsorption–desorption cycles was studied, and the results are shown in Fig. 9. The removal of MB by Fe/SCD-LDH was still over 80% after four times. This showed that the Fe/SCD-LDH adsorbent could be reused frequently without significant loss in adsorption performance. Considering the small reduction in adsorption capacity, this material can be recycled for further use and has great potential for wastewater treatment.

3.2.5. Adsorption kinetics

The adsorption kinetics is an important aspect for controlling the removal process. Since temperature is a highly significant, the kinetics for MB adsorption onto Fe/SCD-LDH at different temperatures was investigated with the help of two kinetic models. Lagergren's pseudo-first-order model and Ho's pseudo-second-order model [27] are most widely used to predict the mechanism of adsorption kinetics.

The pseudo-first-order kinetic model is expressed by the following equation:

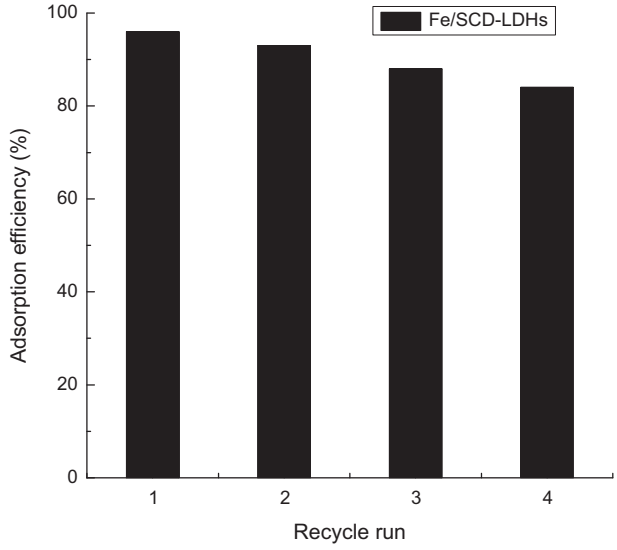

Fig. 9. Reutilization of the adsorption (conditions: volume: 100 mL, adsorbents: 0.1 g, contact time: 5 h; temperature: 303 K, pH 7).

$$Q_t = Q_e(1 - e^{-k_1 t}) \quad (2)$$

This equation may be linearized in this case:

$$\ln(Q_e - Q_t) = \ln Q_e - k_1 t \quad (3)$$

where Q_t and Q_e (mg/g) refer to the amounts of adsorbed MB at time t and at equilibrium, respectively, and k_1 (h^{-1}) is the first-order rate constant.

According to Ho and McKay, the differential equation for pseudo-second-order model is:

$$\frac{t}{Q_t} = \frac{1}{k_2 Q_e^2} + \frac{t}{Q_e} \quad (4)$$

where Q_t and Q_e (mg/g) refer to the amounts of adsorbed MB at time t and at equilibrium, respectively, and k_2 (g/mg h) is the pseudo-second-order rate constant.

The adsorption data obtained by experiments have been analyzed using the linear forms of pseudo-first-order model and pseudo-second-order model. The values of Q_e and k_1 were determined from the intercept and slope of the linear plots of Q_t vs. t (Fig. 10(A)). The slope and intercept of the plot of t/Q_t vs. t were used to calculate the second-order rate constant, k_2 (Fig. 10(B)). The corresponding kinetic parameters k_1, k_2, and the correlation coefficient (R^2) are shown in Table 3. The values of R^2 for pseudo-second-order model were higher than those of pseudo-first-order model. Moreover, the calculated equilibrium adsorption capacity ($Q_{e,cal}$) of pseudo-second-order model were consistent with the experimental data. Thus, it was deduced that the pseudo-second-order adsorption mechanism was predominant, and that the overall rate of the MB adsorption process appeared to be controlled by the chemisorption process. Besides, the adsorbed amount of MB at 303 K was higher than other conditions.

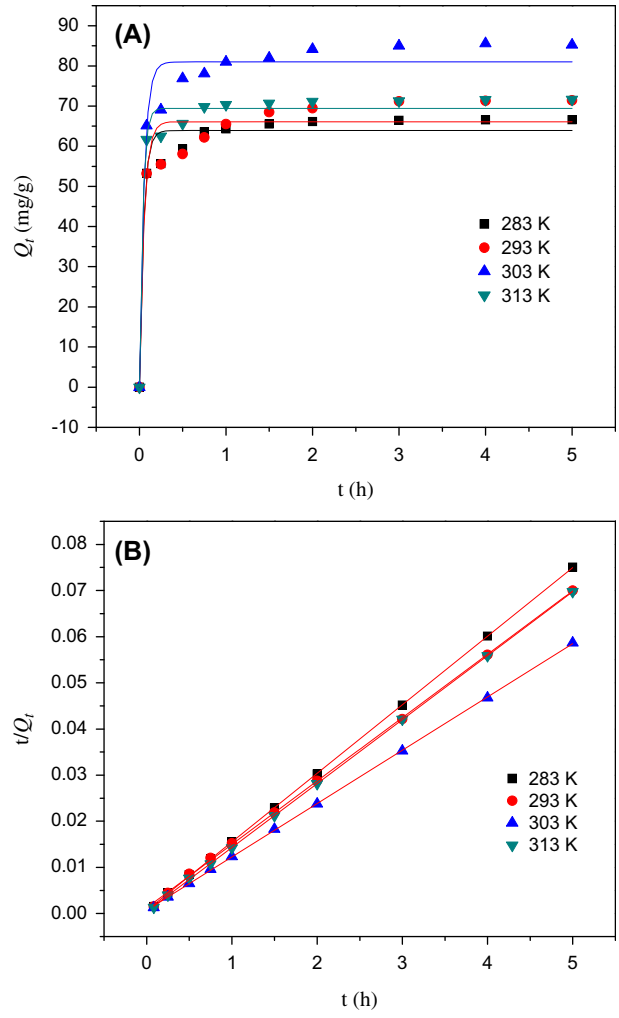

Fig. 10. Effect of temperature on the kinetics for MB removal by Fe/SCD-LDH: (A) first-order kinetics model, (B) pseudo-second-order kinetics model (conditions: volume: 100 mL, adsorbents: 0.1 g, initial MB concentration: 120 mg/L, pH 7).

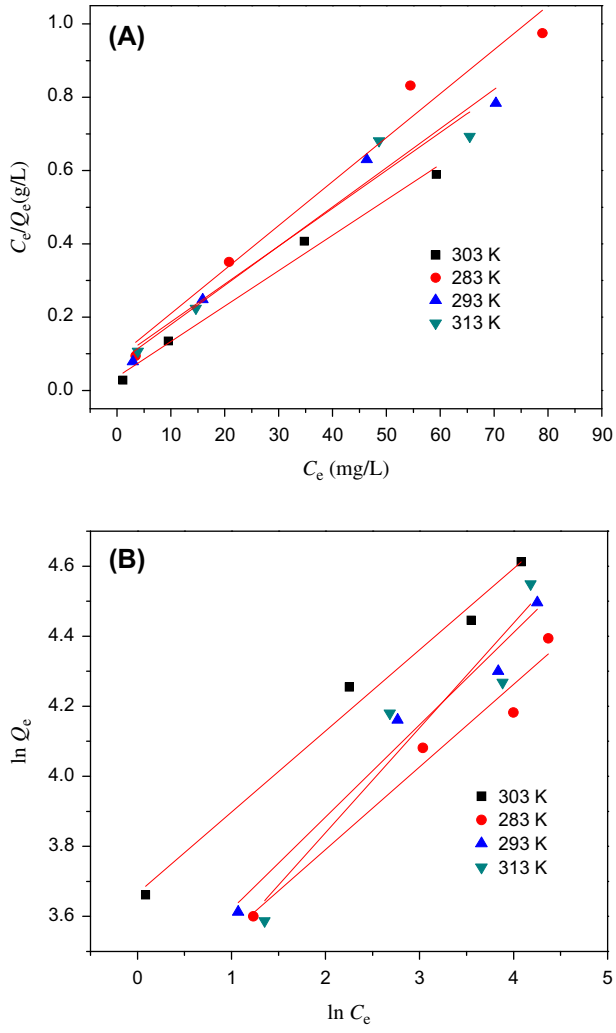

Fig. 11. (A) Langmuir plot illustrating the linear dependences of C_e/Q_e on C_e and (B) Freundlich plot illustrating the linear dependences of ln Q_e on ln C_e (conditions: volume: 100 mL, adsorbents: 0.1 g, pH 7, temperature: 303 K).

3.2.6. Adsorption isotherm and thermodynamic studies

The equilibrium isotherms for the adsorption of MB by Fe_3O_4/SCD-LDH were shown in Fig. 11. For liquid–solid system, the Langmuir equilibrium model is always used, which is based on the assumption that adsorption occurs on a homogenous surface, indicating that a monolayer of dye molecules is adsorbed onto energy sites of the adsorbent surface. Once an adsorbent site is occupied by a dye molecule, no further adsorption can occur at that site [28]. The Langmuir equation can be expressed as:

$$\frac{C_e}{Q_e} = \frac{C_e}{Q_{max}} + \frac{1}{Q_{max} K_L} \tag{5}$$

where Q_e (mg/g) is the amount of MB removed at equilibrium, Q_{max} (mg/g) is the maximum adsorption capacity, C_e (mg/L) is the equilibrium MB concentration, and K_L (L/mg) is the Langmuir constant, which is related to the free energy of adsorption.

The Freundlich equation is an empirical equation used to describe heterogeneous adsorption systems [29]. The linearized equation can be represented as follows:

$$\ln Q_e = \ln K_F + \frac{1}{n} \ln C_e \tag{6}$$

where Q_e and C_e are defined as above, K_F is the Freundlich constant, and n is the heterogeneity factor. The values of Q_{max} and K_L were determined from the slope and intercept of the linear plots of C_e/Q_e vs. C_e (Fig. 11(A)) and the values of K_F and $1/n$ were determined from the slope and intercept of the linear plot of ln Q_e vs. ln C_e (Fig. 11(B)). The isotherm parameters are shown in Table 4. The values of R^2 for Langmuir equilibrium model were higher than those of Freundlich model, indicating that the adsorption process fitted well with Langmuir equilibrium model. The Q_{max} calculated was about 80–100 mg/g. At the same time, when the temperature was 303 K, the Q_{max} reached the highest.

A separation factor R_L is often introduced to evaluate the shape of the Langmuir isotherm and the nature of adsorption; it can be expressed as follows:

Table 3
Kinetic parameters for the adsorption experiments

		Pseudo-first-order			Pseudo-second-order		
T (K)	$Q_{e,exp}$ (mg/g)	$Q_{e,cal}$ (mg/g)	k_1 (h^{-1})	R^2	$Q_{e,cal}$ (mg/g)	k_2 (g/mg h)	R^2
283	66.6	63.91	20.77	0.9671	67.25	23.22	0.9999
293	71.41	66.12	18.42	0.9264	72.83	10.90	0.9997
303	85.26	81.02	18.51	0.9607	86.50	16.57	0.9999
313	71.67	69.44	25.95	0.9799	72.10	33.23	0.9999

Table 4
Adsorption isotherm parameters of MB onto Fe/SCD-LDH

	Langmuir isotherm model				Freundlich isotherm model		
T (K)	K_L (L/mg)	Q_{max} (mg/g)	R^2	R_L	K_F	n	R^2
283	0.133	83.40	0.961	0.045–0.158	27.623	4.24	0.953
293	0.146	93.63	0.972	0.041–0.146	28.693	3.796	0.961
303	0.261	103.5	0.984	0.023–0.087	39.080	4.312	0.980
313	0.127	96.90	0.925	0.047–0.165	25.525	3.341	0.868

$$R_L = \frac{1}{1 + K_L C_0} \quad (7)$$

where C_0 (mg/L) is the initial MB concentration and K_L is the adsorption constant of the Langmuir isotherm (L/mg). The value of R_L is related to the shape of the isotherms to be either unfavorable ($R_L > 1$), linear ($R_L = 1$), favorable ($0 < R_L < 1$), or irreversible ($R_L = 0$) [30]. The calculated value of R_L in the range of 0–1 (Table 4) confirmed the favorable uptake of MB by Fe/SCD-LDH.

4. Conclusions

We have successfully synthesized Fe/SCD-LDH nanoparticles with the properties of superparamagnetism and inclusion properties of SCD. The interlayer SCD of MgAl-NO_3 LDH is confirmed by FT-IR, XRD, and EDX. MB could be recovered fast and efficiently from the aqueous solution using the as-synthesized magnetic nanoadsorbents. SEM and BET investigations confirmed that Fe/SCD-LDHs possessed high crystallinity, hierarchical structure as well as large specific surface area. The efficiency of Fe/SCD-LDH as an adsorbent to remove MB from aqueous solution was studied. It was found that MB could be removed effectively by optimizing experimental conditions. The adsorption of MB on Fe/SCD-LDH was found to be pH dependent. The kinetics of adsorption was well described by the pseudo-second-order kinetics model. The Langmuir isotherm was found to fit the data of equilibrium experiments well. All results indicated that Fe/SCD-LDH could be used as a low-cost and alternative adsorbent for the removal of cationic pollutants from wastewaters.

Acknowledgments

The authors would like to thank National Natural Science Foundation of China (No. 21476269) and Provincial Natural Science Foundation of Hunan (No. 14JJ2014) for the financial supports of this work.

References

[1] A. Latif, S. Noor, Q.M. Sharif, M. Najeebullah, Different techniques recently used for the treatment of textile dyes effluents: A review, J. Chem. Soc. Pak. 32 (2010) 115–124.
[2] T. Robinson, G. McMullan, R. Marchant, P. Nigam, Remediation of dyes in textile effluent: A critical review on current treatment technologies with a proposed alternative, Bioresour. Technol. 77 (2001) 247–255.
[3] J. Rouquerol, F. Rouquerol, P. Llewellyn, G. Maurin, K. Sing, Adsorption by Powders and Porous Solids, second ed., Academic Press, Amsterdam, 2014.
[4] D.D. Do, Adsorption science and technology, Proceedings of the Second Pacific Basin Conference on Adsorption Science and Technology, World Scientific, Brisbane, 2000
[5] V. Rives, M. del Arco, C. Martín, Intercalation of drugs in layered double hydroxides and their controlled release: A review, Appl. Clay Sci. 88–89 (2014) 239–269.
[6] F. Cavani, F. Trifirò, A. Vaccari, Hydrotalcite-type anionic clays: Preparation, properties and applications, Catal. Today 11 (1991) 173–301.
[7] L. Lv, J. He, M. Wei, D.G. Evans, Z. Zhou, Treatment of high fluoride concentration water by MgAl-CO_3 layered double hydroxides: Kinetic and equilibrium studies, Water Res. 41 (2007) 1534–1542.
[8] S.W. Rhee, M.J. Kang, H. Kim, C.H. Moon, Removal of aquatic chromate ion involving rehydration reaction of calcined layered double hydroxide (Mg-Al-CO_3), Environ. Technol. 18 (1997) 231–236.
[9] X. Kong, S. Shi, J. Han, F. Zhu, M. Wei, X. Duan, Preparation of Glycy-l-Tyrosine intercalated layered double hydroxide film and its *in vitro* release behavior, Chem. Eng. J. 157 (2010) 598–604.
[10] J. Chakraborty, S. Roychowdhury, S. Sengupta, S. Ghosh, Mg–Al layered double hydroxide–methotrexate nanohybrid drug delivery system: Evaluation of efficacy, Mater. Sci. Eng.: C 33 (2013) 2168–2174.
[11] L.C. Hsu, S.L. Wang, Y.M. Tzou, C.F. Lin, J.H. Chen, The removal and recovery of Cr(VI) by Li/Al layered double hydroxide (LDH), J. Hazard. Mater. 142 (2007) 242–249.

[12] H. Zaghouane-Boudiaf, M. Boutahala, L. Arab, Removal of methyl orange from aqueous solution by uncalcined and calcined MgNiAl layered double hydroxides (LDHs), Chem. Eng. J. 187 (2012) 142–149.
[13] V. Rives, M. del Arco, C. Martín, Layered double hydroxides as drug carriers and for controlled release of non-steroidal antiinflammatory drugs (NSAIDs): A review, J. Controlled Release 169 (2013) 28–39.
[14] F. Zhang, X. Xiang, F. Li, X. Duan, Layered double hydroxides as catalytic materials: Recent development, Catal. Surv. Asia 12 (2008) 253–265.
[15] B.M. Choudary, S. Madhi, N.S. Chowdari, M.L. Kantam, B. Sreedhar, Layered double hydroxide supported nanopalladium catalyst for Heck-, Suzuki-, Sonogashira-, and Stille-Type coupling reactions of chloroarenes, J. Am. Chem. Soc. 124 (2002) 14127–14136.
[16] Y. Zhao, M. Wei, J. Lu, Z.L. Wang, X. Duan, Biotemplated hierarchical nanostructure of layered double hydroxides with improved photocatalysis performance, ACS Nano 3 (2009) 4009–4016.
[17] T. Yang, Poly(vinyl alcohol)/sulfated β-cyclodextrin for direct methanol fuel cell applications, Int. J. Hydrogen Energy 34 (2009) 6917–6924.
[18] M. Meyn, K. Beneke, G. Lagaly, Anion-exchange reactions of layered double hydroxides, Inorg. Chem. 29 (1990) 5201–5207.
[19] F. Jiao, J. Yu, H. Song, X. Jiang, H. Yang, S. Shi, X. Chen, W. Yang, Excellent adsorption of Acid Flavine 2G by MgAl-mixed metal oxides with magnetic iron oxide, Appl. Clay Sci. 101 (2014) 30–37.
[20] Z.P. Xu, G.Q. Lu, Hydrothermal synthesis of layered Double hydroxides (LDHs) from mixed MgO and Al_2O_3: LDH formation mechanism, Chem. Mater. 17 (2005) 1055–1062.
[21] J. Wang, M. Wei, G. Rao, D.G. Evans, X. Duan, Structure and thermal decomposition of sulfated *β*-cyclodextrin intercalated in a layered double hydroxide, J. Solid State Chem. 177 (2004) 366–371.
[22] X. Xue, Q. Gu, G. Pan, J. Liang, G. Huang, G. Sun, S. Ma, X. Yang, Nanocage structure derived from sulfonated β-cyclodextrin intercalated layered double hydroxides and selective adsorption for phenol compounds, Inorg. Chem. 53 (2014) 1521–1529.
[23] M. Wei, J. Wang, J. He, D.G. Evans, X. Duan, In situ FT-IR, *in situ* HT-XRD and TPDE study of thermal decomposition of sulfated *β*-cyclodextrin intercalated in layered double hydroxides, Microporous Mesoporous Mater. 78 (2005) 53–61.
[24] F. Jiao, H. Song, W. Yang, X. Jiang, X. Chen, J. Yu, Enantioselective separation of tryptophan by Mg–Al layered double hydroxides intercalated with tartaric acid derivative, Appl. Clay Sci. 75–76 (2013) 92–99.
[25] J.S. Valente, F. Tzompantzi, J. Prince, J.G.H. Cortez, R. Gomez, Adsorption and photocatalytic degradation of phenol and 2,4 dichlorophenoxiacetic acid by Mg–Zn–Al layered double hydroxides, Appl. Catal. B: Environ. 90 (2009) 330–338.
[26] E. Borghi, M. Occhiuzzi, E. Foresti, I.G. Lesciand, N. Roveri, Spectroscopic characterization of Fe-doped synthetic chrysotile by EPR, DRS and magnetic susceptibility measurements, Phys. Chem. Chem. Phys. 12 (2010) 227–238.
[27] Y.S. Ho, G. McKay, A comparison of chemisorption kinetic models applied to pollutant removal on various sorbents, Proc. Saf. Environ. Prot. 76 (1988) 332–340.
[28] Y.S. Ho, G. McKay, Pseudo-second order model for sorption processes, Process Biochem. 34 (1999) 451–465.
[29] L. Yu, W. Xue, L. Cui, W. Xing, X. Cao, H. Li, Use of hydroxypropyl-*β*-cyclodextrin/polyethylene glycol 400, modified Fe_3O_4 nanoparticles for congo red removal, Int. J. Biol. Macromol. 64 (2014) 233–239.
[30] A.Z.M. Badruddoza, G.S.S. Hazel, K. Hidajat, M.S. Uddin, Synthesis of carboxymethyl-*β*-cyclodextrin conjugated magnetic nano-adsorbent for removal of methylene blue, Colloids Surf., A 367 (2010) 85–95.